

# Generic Evolving Self-Organizing Neuro-Fuzzy Control of Bio-inspired Unmanned Aerial Vehicles

Md Meftahul Ferdous, *Student Member, IEEE*, Mahardhika Pratama, *Member, IEEE*, Sreenatha G. Anavatti, Matthew A. Garratt, and Yongping Pan

**Abstract**—At recent times, with the incremental demand of the fully autonomous system, a huge research interest is observed in learning machine based intelligent, self-organizing, and evolving controller. In this work, a new evolving and self-organizing controller namely Generic-controller (G-controller) is proposed. The G-controller that works in the fully online mode with very minor expert domain knowledge is developed by incorporating the sliding model control (SMC) theory based learning algorithm with an advanced incremental learning machine namely Generic Evolving Neuro-Fuzzy Inference System (GENEFIS). The controller starts operating from scratch with an empty set of fuzzy rules, and therefore, no offline training is required. To cope with the plant's vulnerable behavior, the controller can add, or prune the rules on demand. Control law and adaptation laws for the consequents are derived from the SMC algorithm to establish a stable closed-loop system, where the stability of the G-controller is guaranteed using the Lyapunov function. The uniform asymptotic convergence of tracking error to zero is witnessed through the implication of an auxiliary robustifying control term. In addition, the implementation of the multivariate Gaussian function helps the controller to handle the non-axis parallel data from the plant and consequently enhances the robustness against the uncertainties and environmental perturbations. Finally, the controller's performance has been evaluated by observing the tracking performance in controlling simulated plants of unmanned aerial vehicle namely bio-inspired flapping wing micro air vehicle (BIFW MAV) and hexacopter for a variety of trajectories.

**Index Terms**—Data-driven controller, Evolving, GENEFIS, Model-free, Neuro-fuzzy, Self-constructing, Sliding mode control

## I. INTRODUCTION

**I**N AUTONOMOUS unmanned vehicle systems, to obtain an accurate first principle based model is considerably arduous due to their highly non-linear and over-actuated or under-actuated behavior. Besides, various uncertainty factor like impreciseness in the obtained data from sensors, induced noise by the sensors, outdoor environmental uncertainties like

wind gust, motor degradation, etc. are strenuous or impossible to integrate into the first principle models. In such circumstances, approaches without the necessity of accurate mathematical models of the system under control, are much appreciated. Being a model-free approach, the Neural Network (NN) and Fuzzy Logic system (FLS) based controllers have been successfully implemented in many control applications [1], [2], [3], [4] over the past few years. Recently, systems with an amalgamation of FLS and NN namely Fuzzy Neural Network (FNN) based controllers are becoming popular in a variety of engineering application, such as in controlling robot manipulator [5], anti-lock braking systems [6], temperature control [7], controlling motor drive [8], direct current converter [9] etc.

To develop an FLS, NN, or an FNN controller with a better accuracy, is challenging. There exist numerous methods to develop FLS, NN, or FNN controllers [10], [11], [12]. When the system dynamics and various characteristics of a plant to be controlled are known, then the information is utilized to train the controller. It constructs a fixed-structured controller with a certain number of rules, membership functions, neurons, and layers. Due to the fixed structure, these controllers cannot cope with changing plant dynamics. Similarly, during online control application, the plant dynamics and other system information are not readily available. Therefore, the fixed-structured FLS, NN, or FNN controller become unreliable. Furthermore, the characteristic of real-world plants is non-stationary. This should not be handled by a fixed-size controller. To handle uncertainties in control system, researchers have tried to combine the FLS, NN, FNN system with sliding mode control (SMC) [13],  $H_\infty$  control, back-stepping, etc. Such amalgamation empowers the FLS, NN, FNN controller with the feature of tuning parameters, which provides a more robust and adaptive control structure. It assists them to mitigate the adverse effects of various uncertainties and perturbations. However, such adaptive FNN control structures are not able to evolve their structures by adding or pruning rules. It forces the controller to determine the number of rules a priori, where a selection of few fuzzy rules may hinder to achieve adequate and desired control performance. On the other hand, consideration of too many rules may create complexity, or make it impossible to implement in real time.

The problems mentioned above can be circumvented by implementing evolving FLS, NN, FNN controllers that can evolve their structure by adding, or deleting rules through self-organizing techniques. In recent time, researchers are trying to develop evolving FLS, NN, FNN controllers by following

Md Meftahul Ferdous is with the School of Engineering and Information Technology, University of New South Wales at the Australian Defence Force Academy, Canberra, ACT 2612, Australia, e-mail: m.ferdous@unsw.edu.au.

Mahardhika Pratama is with the School of Computer Science and Engineering, Nanyang Technological University, Singapore, 639798, Singapore, e-mail: mpratama@ntu.edu.sg.

Sreenatha G. Anavatti is with the School of Engineering and Information Technology, University of New South Wales at the Australian Defence Force Academy, Canberra, ACT 2612, Australia, e-mail: s.anavatti@adfa.edu.au.

Matthew A. Garratt is with the School of Engineering and Information Technology, University of New South Wales at the Australian Defence Force Academy, Canberra, ACT 2612, Australia, e-mail: M.Garratt@adfa.edu.au.

Yongping Pan is with the Department of Biomedical Engineering, National University of Singapore, Singapore, e-mail: biepany@nus.edu.sg.

various approaches to add or delete the rules [14]. In the rule growing mechanism in [15],  $\epsilon$ -completeness and system error was measured to add a rule, and the concept of error reduction ratio (ERR) was utilized to prune a rule. Therefore, their developed self-organizing FNN controller can adapt both the parameters and the structure. Nevertheless, the computation of larger matrix in each step, and storing of all previous input-output data makes their proposed technique computationally costly. Sometimes, the spatial proximity between a particular data-point and all other points, namely potential is used to add or replace a rule in an evolving fuzzy controller as described in [16]. However, the controller proposed in [16] cannot prune any rules, which makes them computationally costly in real-time control, especially in case of controlling highly nonlinear over-actuated complex systems. Researchers have also tried in [17] to employ a max-min method to add and prune layers, and error backpropagation to tune evolving neuro-fuzzy controller's parameters like weight, center, and width of Gaussian membership function. Nonetheless, the controller needed some knowledge about the plant like the bounded nominal matrix, which may not be known during control operation.

Besides, an evolving TS fuzzy controller can be developed by combining it with a fixed TS fuzzy FLS as exposed in [18], where the evolving TS FLS worked online, and no previous information was needed. Though such design of an evolving controller is simple, it requires some information about the plant due to the utilization of static TS fuzzy system. Researchers have tried to develop a cloud-based evolving fuzzy controller in [19]. The advantage of their cloud-based evolving fuzzy controller was the parameter-free antecedent part of a rule, whereas the consequent part was expressed in the form of a PID controller. The three parameters of their PID like evolving controller were tuned online through Lyapunov theory based stable adaptation law. The controller can add rules or clouds by measuring local data density. Their evolving structure helped them to track the desired trajectory properly. However, they were not able to delete rules, or clouds. An evolving fuzzy controller is possible to develop by using Fuzzy granular computation in explained [20], which can model and control an unknown non-stationary system in online without any experts knowledge. A fuzzy Lyapunov function was utilized to evaluate the closed-loop stability of their controller. Data uncertainty was handled and incorporated into knowledge domain by Fuzzy granular computation. However, diversity in data among different granules, and unmeasurable state variables was not considered.

Furthermore, an evolving neuro-fuzzy controller can also be developed by utilizing model predictive control methods as described in [21], [22], [23]. A radial basis function neural network based self-organizing controller was developed in [21] where the evolving neuro-fuzzy system was utilized to bound the modeling error uniformly for nonlinear systems. Besides, a fast gradient method was employed to minimize the computational cost of their online evolving model predictive control method. The Lyapunov theory demonstrated the closed-loop stability of their control method. However, their controller was not implemented in real-time application.

Until now, all the discussed evolving controllers have utilized univariate Gaussian function, which does not expose the scale-invariant property. Besides, they are not effective in dealing with non-axis parallel data distribution. To mitigate these shortcomings, we utilized a multivariate Gaussian functions based incremental learning machine algorithm called generic evolving neuro-fuzzy inference system (GENEFIS) [24]. In this work, GENEFIS is amalgamated with SMC technique to develop a self-evolving controller namely G-controller. In this work, main features of the proposed G-controller are as follows:

- 1) The controller's performance does not depends upon the plant dynamics or any other features of the plant.
- 2) No previous information or off-line training is required. Thus, the controller starts self-construction from scratch with only one rule at the beginning, and then it adds, deletes, or merge rules to follow the desired trajectory. Besides, the application of a fast kernel-based metric approach helps to capture fuzzy set and rule level redundancy.
- 3) Integration of the Generalized Adaptive Resonance Theory+ (GART+) helps to upgrade the premise parameters with respect to input data distributions, and utilization of multivariate Gaussian function aids the controller to handle a variety of data generated from the sudden change in plants, or from uncertainties, environmental perturbations.
- 4) Adaptation law for the GENEFIS based G-controller's consequent parameters are derived from the SMC learning theory, which confirms a stable closed-loop control system. A robustifying auxiliary control term ensures uniform asymptotic convergence of tracking error to zero. Finally, the stability of the G-controller is proved using the Lyapunov function.
- 5) Successful evaluation of the proposed G-controller through implementing it into the simulated BIFW MAV, and hexacopter plant.

The above-mentioned characteristics of the proposed self-evolving G-controller make them an appropriate candidate to control autonomous vehicles like BIFW MAV, quadcopter, hexacopter, octocopter with better accuracy than a stand-alone first principle based controller. Furthermore, the whole controller is developed using C programming language to make it compatible with all types of hardware, where their implementation is made publicly available in [25]. In the next subsection I-A, the recent implementation of FLS, NN, FNN based controller in autonomous vehicles are summarized.

#### A. Related Work

Autonomous vehicles express a complex mathematical model, where the incorporation of various uncertainties is very difficult, or not possible in some cases. The situation becomes worse, when those vehicles are highly nonlinear, under-actuated, or over-actuated like bio-inspired flapping wing micro air vehicle (BIFW MAV), quadcopter, hexacopter, octocopter unmanned aerial vehicles [26]. It is due to the associated uncertainties, and rarely available information or

no information at all about the autonomous vehicles. As a consequence, in recent time research interest is increasing in employing model-free adaptive and self-evolving fuzzy and neuro-fuzzy controller to autonomous vehicles. A self-organizing adaptive fuzzy controller was developed in [27] to control a complex surface vehicle with uncertainties, and external perturbation. A robustifying auxiliary control term contributed to ensure closed-loop system stability of their controller. From simulation studies, better performance was observed from their fixed adaptive control techniques. However, a higher number of rules were generated to achieve desired tracking accuracy. In [28], an adaptive fuzzy-PID controller was developed to control the attitude and altitude of a quadrotor. Though the TS-fuzzy system can approximate the plant's dynamics with uncertainties and unknown disturbances, their dependency of a static PID controller affected their performance to cope with sudden changes in plant dynamics.

An evolving fuzzy reference controller was proposed in [29], which can partition the input-output space. It was able to identify the local controllers gain. The stability of their controller is yet to prove. In [30], self-tuning of a two-degrees-of-freedom control algorithm was proposed based on an evolving fuzzy model. Their control algorithm consisted of a feedforward, and feedback loop. The feedforward part was derived from inversion of TS fuzzy model, which helped the system to follow the trajectory closely. An evolving fuzzy system with the ability to add, prune, merge, or split the clusters was utilized in the feedback loop of their controller. Nonetheless, their controller was applicable for single-input-single-output (SISO) systems only. In [31], a Taylor Series Neuro Fuzzy (TaSe-NF) model based online self-evolving neuro fuzzy controller is developed. The local online learning of consequent parameters provided them a proper control mechanism, and the self-evolving structure provided satisfactory performance with minimum rules and no prior information about the plant. However, their controller's stability yet to be proved.

A direct evolving neural controller was developed in [32] by implementing a self-constructing radial basis function neural network (RBFNN), which can add or prune neurons online to adapt to plant condition. The closed-loop stability of their controller was guaranteed by Lyapunov stability theory. A self-organizing fuzzy controller is proposed in [33], where the consequents are adapted at each selected topology, and membership functions were added online. After analysing the complete operating region of the plant the topology was modified, which raised their controllers robustness. However, their controller had a dependency of plants sampling period, which made them impractical in implementing real embedded UAV plants.

An interval type-2 fuzzy neural network based gain adaptive sliding mode controller was developed in [34] to control the attitude micro aerial vehicle. The sliding mode gain adaptive law was utilized to tune the parameters of the interval type-2 fuzzy neural network online. Better tracking accuracy was observed than the conventional adaptive sliding mode controller. However, the fuzzy controller can only tune its parameters, and unable to evolve their structure by adding or

deleting rules. A self-organizing interval type-2 fuzzy neural network (SOIT2FNN) based controller was developed in [35], and combined with a PD controller to control the attitude of a quadcopter Micro Aerial Vehicle (MAV), where the SOIT2FNN was able to learn the inverse model of quadcopter online. Besides, it could minimize the model errors and external disturbances. Nonetheless, due to their dependency on static PD controller, they were affected by sudden changes in plant dynamics.

To deal with the uncertainties exists in the nonlinear complex FW MAV model, a radial basis function neural network (RBFNN) was utilized in [36]. The stability of their closed loop control system was verified through Lyapunov stability theorem. By selecting appropriate control variables, a good trajectory tracking performance was observed from their simulation results. However, their control technique was not self-evolving in nature. A fuzzy controller namely hybrid adaptive fuzzy controller (HAFC) was developed in [14] to control a dragonfly-like FW MAV. Their HAFC was able to tune its parameters by using the hybrid adaptive law to minimize the tracking error. The simulation results of the HAFC were compared with a direct adaptive (DA) method based fuzzy controller (DAFC). Better tracking performance was observed from the HAFC than the DAFC. However, their controller was constructed by the batch learning process, therefore static in nature. A Spiking Neural Network (SNN) based controller was developed for an FW MAV called RoboBee in [37], where they had utilized a reward-modulated Hebbian plasticity mechanism to adopt a leaky integrate-and-fire spiking neural network in flight. In [38], an online self-organizing neural controller was combined with a conventional controller to track the desired trajectory of a simulated helicopter plant, while performing highly nonlinear maneuvers. In their dynamic radial basis function network, a Lyapunov based adaptation law was integrated with the neuron growing and pruning mechanism, which ensured the closed-loop stability and desired tracking accuracy. A self-constructing neuro-fuzzy controller was proposed in [39] to track the desired attitude of a quadcopter, which can add, and delete rules online. Integration of a projection based adaptation law handled the drift, and singularity problem in antecedent parameters. However, due to their rule growing mechanism comparatively higher number of rules were generated online, which made them computationally costly.

To adapt the consequent parameters of various self-evolving neuro-fuzzy controllers, sometimes gradient-based algorithms are utilized. These gradient-based algorithms perform better only with those plants, where a slow variation in their dynamics is observed. Besides, some gradient-based algorithms namely dynamic backpropagation includes partial derivatives, which may slow down the convergence speed, especially in case of complex search space. In addition, the tuning procedure may be trapped into a local minimum in backpropagation methods as explained in [40]. As a solution to these problems, evolutionary approaches are proposed in [41]. However, the stability of such controller is questionable. To overcome these issues, sliding mode control (SMC) theory based algorithms were proposed to tune the consequent parameter of various

FLS, NN, FNNs in [42], [43], [44], [45]. An SMC theory based adaptive and online neuro-fuzzy-PID controller was developed in [46], which exhibited an improved performance than standalone PID controller. Since the adaptation laws are derived from the PID controller part, without the PID controller, the neuro-fuzzy controller was unable to tune its parameters.

To mitigate the shortcomings of the existing self-evolving neuro-fuzzy controller, in this work a novel self-evolving controller namely G-controller is developed in guiding various autonomous vehicles. The evolving architecture of the controller is inspired by the incremental learning algorithm called GENEFIS [24], and the consequent parameters are adapted utilizing SMC theory based learning algorithm. Unlike the evolving neuro-fuzzy controllers discussed in the literature, the integration of GART+ with a four-stage checking to evolve rules provide a very quick response, and reduce the computational complexity by pruning unnecessary rules. Instead of predefined values, the sliding parameters in the SMC theory is also self-organizing in this work. To the best of our knowledge, such evolving sliding parameters are never utilized before in any of the existing evolving neuro-fuzzy controllers.

The organization of rest of this paper is as follows. Section II describes the problem associated with two autonomous vehicles namely BIFW MAV, and hexacopter in tracking the trajectory accurately. The self-evolving architecture of the GENEFIS based G-controller is explained in Section III. Section IV represents SMC learning algorithm based adaptation of the proposed G-controller. The results are summarized, and analysed in Section V. Finally, the paper ends with the concluding remarks encompassed in Section VI.

## II. PROBLEM STATEMENT

Modelling and control of BIFW MAV is one of the latest research topics related to the field of autonomous Unmanned Aerial Vehicles (UAVs). BIFW MAV exhibits some advanced characteristics like fast flight, vertical take-off and landing, hovering, and quick turn, and enhanced manoeuvrability when compared to similar sized fixed and rotary wing UAVs. To observe these features from a BIFW MAV, an advanced control mechanism is a must need. To take the challenge, our proposed G-controller is implemented in a bio-inspired (BI) dragonfly-like four wings simulated MAV plant developed by the Defence Science and Technology Group (DSTG) as described in [47]. The simulated BIFW MAV plant saves the time and expenses to set-up for experimental flight test. The high level architecture of the BIFW MAV flight simulator is exposed in Fig. 1.

In the flight simulator, four actuators are denoted by 'Actuator 1', 'Actuator 2', 'Actuator 3', and 'Actuator 4' as shown in Fig. 1. These actuators are utilized to control four wings of the BIFW MAV. Each actuator is controlled by eight (8) flapping parameters indicated by F1 to F8 in 'flapping parameters' block, where F1 indicates the stroke plane angle (in rad), F2 is the flapping frequency (in Hz), F3 represents the flapping

Table I  
EFFECTS OF FLAPPING PARAMETERS IN DIFFERENT MANOEUVRING OF FW MAV( $\phi_0$ : FLAPPING AMPLITUDE(DEGREE);  $\Psi$ : PHASE(DEGREE))

Actuators with corresponding flapping parameter	Action
Actuator: 1, 2, 3, 4; $\phi_0$ : 90	Take-off
Actuator: 1, 2; $\phi_0$ : 90 and Actuator: 3, 4; $\phi_0$ : 60	Roll-right
Actuator: 1, 2; $\phi_0$ : 60 and Actuator: 3, 4; $\phi_0$ : 90	Roll-left
Actuator: 1, 3; $\phi_0$ : 90 and Actuator: 2, 4; $\phi_0$ : 60	Pitch-up
Actuator: 1, 3; $\phi_0$ : 60 and Actuator: 2, 4; $\phi_0$ : 90	Pitch-down
Actuator: 1, 4; $\Psi$ : 90 and Actuator: 2, 3; $\Psi$ : 60	Yaw-right
Actuator: 1, 4; $\Psi$ : 60 and Actuator: 2, 3; $\Psi$ : 90	Yaw-left

amplitude (in rad), F4 presents the mean angle of attack (in rad), F5 is the amplitude of pitching oscillation (in rad), F6 is the phase difference between the pitching and plunging motion, F7 is the time step (in sec), F8 is the kappa set as zero in the plant. By altering these flapping parameters, from this flight simulator various mission profile or manoeuvrability such as take-off, rolling, pitching, and yawing of an BIFW MAV can be analysed. To find the dominant flapping parameter, a parametric analysis is accomplished in this work. It is found that the flapping amplitude is the most dominant among the eight parameters to control the BIFW MAV. By tuning the flapping amplitude the take-off, rolling, and pitching motion is observed. Only for the yawing motion flapping phase needs to be tuned. Tuning of these parameters and their effect on various manoeuvring is summarized in TABLE I.

The force generated by each actuator ( $F_{r_i}$ ) is supplied to the 'Forces & Moments' block of the Fig. 1. Besides the four forces from four actuators ( $F_{r_1}$ ,  $F_{r_2}$ ,  $F_{r_3}$ ,  $F_{r_4}$ ), the mass and Direction Cosine Matrix (DCM) is also fed to the 'Forces & Moments' block. This block supplies the required force (F) and moment (M) to the rigid body dynamics of the simulator based on the relative airflow acting on each wing and the commanded actuator speed. The wing kinematics were modelled utilizing the derivation explained in [48], [49], [50], where it was considered that the wing was flapping in an inclined stroke plane with a certain angle. In the simulator, to express the MAV's flapping profile the flapping angle ( $\phi$ ) is presented in a sinusoidal form as follows:

$$\phi(t) = \phi_a \cos(\pi f t) \quad (1)$$

where  $\phi_a$  is the flapping amplitude in radian,  $f$  is the flapping frequency in Hz,  $t$  is the time in second. Besides, the angle of attack ( $A_{aoa}$ ) can be expressed as:

$$A_{aoa} = A_{mn} - A_p \sin(\omega dt + \Psi) \quad (2)$$

where  $A_{mn}$  is mean angle of attack in radian,  $A_p$  is amplitude of pitching oscillation in radian,  $dt$  is time step in seconds, and  $\Psi$  is the phase difference between the pitching and plunging motion. All the four wings of the BIFW MAV follows the same flapping profile.

Now in the 'Forces & Moments' block  $M$  is actually a summation of four momentums of four different actuators, which can be expressed as:

$$M = M_1 + M_2 + M_3 + M_4 \quad (3)$$

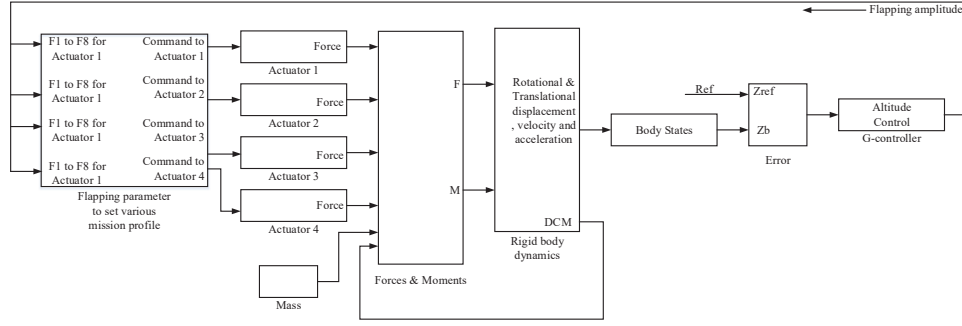


Figure 1. High level architecture of the over-actuated FWMAV plant

Each of these moments ( $M_1, M_2, M_3, M_4$ ) is actually the torque induced in each wing based on the relative airflow acting on each of them. The individual momentum of each wing can be expressed as:

$$M_1 = F_{r_1} \times (CG - CP_1) \quad (4)$$

$$M_2 = F_{r_2} \times (CG - CP_2) \quad (5)$$

$$M_3 = F_{r_3} \times (CG - CP_3) \quad (6)$$

$$M_4 = F_{r_4} \times (CG - CP_4) \quad (7)$$

where,  $CG = [0 \ 0 \ 0]$ ; and  $CP_1 = [0.08 \ 0.05 \ 0]$ ;  $CP_2 = [0.08 \ 0.05 \ 0]$ ;  $CP_3 = [0.08 \ -0.05 \ 0]$ ;  $CP_4 = [-0.08 \ -0.05 \ 0]$ ; and  $\times$  is presenting  $(3 \times 3)$  cross product. Each of the forces ( $F_{r_i}$ ) are three dimensional where the elements are  $[F_{xr} \ F_{yr} \ F_{zr}]$ . On the other hand,  $F$  is actually a summation of four forces of four different actuators along with the gravitational force, which can be expressed as:

$$F = F_{r_1} + F_{r_2} + F_{r_3} + F_{r_4} + (mg \times DCM) \quad (8)$$

where,  $m$  is the mass,  $g$  is the acceleration due to gravity. Finally, in the 'Rigid Body Dynamics' block the forces and moments are converted into the body coordinate system, and all the required body states like three dimensional rotational displacements (roll( $\phi$ ), pitch( $\theta$ ), yaw( $\psi$ )), velocities ( $\omega_{bx}, \omega_{by}, \omega_{bz}$ ), and accelerations ( $\alpha_{bx} = \frac{d\omega_{bx}}{dt}, \alpha_{by} = \frac{d\omega_{by}}{dt}, \alpha_{bz} = \frac{d\omega_{bz}}{dt}$ ) and translational displacements ( $X_b, Y_b, Z_b$ ), velocities ( $v_{bx}, v_{by}, v_{bz}$ ), and accelerations ( $a_{bx} = \frac{dv_{bx}}{dt}, a_{by} = \frac{dv_{by}}{dt}, a_{bz} = \frac{dv_{bz}}{dt}$ ) are obtained, and the MAV states are updated. The complete mathematical model of the BIFW MAV dynamics is written in C code and MATLAB m file, where the C code is called using Simulink S-function. The complete BIFW MAV simulator with the necessary files describing the dynamics is made publicly available in [25]. In addition, the development of hardware construction of the above described BIFW MAV plant is going on at this moment by the DSTG group. Their developed flapping wing-actuation system is shown in the supplementary document. After successful completion of the construction, our proposed G-controller will be implemented in hardware, since the G-controller is compatible with their hardware.

Besides the BIFW MAV, another autonomous vehicle namely hexacopter, a rotary wing UAV is considered in this

work. The simulated hexacopter plant is developed by UAV laboratory of the UNSW at the Australian Defence Force Academy. The model is of medium fidelity and contains both full 6 degrees of freedom (DOF) rigid body dynamics and non-linear aerodynamics. The hexacopter simulated plant introduces two extra degrees of freedom which are obtained by shifting two masses using two aircraft servos with each mass sliding along its own rail aligned in longitudinal and lateral directions respectively, which makes the plant an over-actuated system. The top-level diagram of this over-actuated simulated plant is exhibited in Fig. 2.

The 'attitude controller' block consists of inner loop and outer loop controllers. In outer loop, our proposed G-controller is utilized and PID is used in inner loop. The altitude or height, the moving-mass based shifting of center of gravity in X and Y axis ( $CG_X$ , and  $CG_Y$ ) is controlled by the G-controller. Therefore, G-controllers are utilized in 'outer loop controller', 'Height controller', ' $CG_X$  controller', ' $CG_Y$  controller' blocks in Fig. 2. The 'control mixing' block converts the attitude (roll and pitch), yaw, and thrust commands coming from the controller to motor speed commands. This is done using a simple linear mixing arrangement based on the relevant positions of each rotor. The 'forces and moments' block calculates the thrust and torque of each rotor based on the relative airflow acting on each rotor and the commanded motor speed. The thrusts and torque of each rotor are then added together to give the total vertical force ( $Fz$ ) and yawing torque ( $N$ ) of the hexacopter. The thrust of each rotor is multiplied by the appropriate moment arms to calculate the rolling ( $L$ ) and pitching moments ( $M$ ) acting on the airframe. The thrust, yawing torque and rolling and pitching moments are then fed to the rigid body dynamics block so that the hexacopter state can be updated. The above explained plant is also being converted into hardware at the UAV laboratory of UNSW@ADFA. The airframe components and basic structure of the hexacopter is exhibited in Fig. 3. After the accomplishment of the construction, our proposed controller will be instrumented in that hardware.

Deriving a proper mathematical model of such highly nonlinear, complex, and over-actuated micro air vehicles are

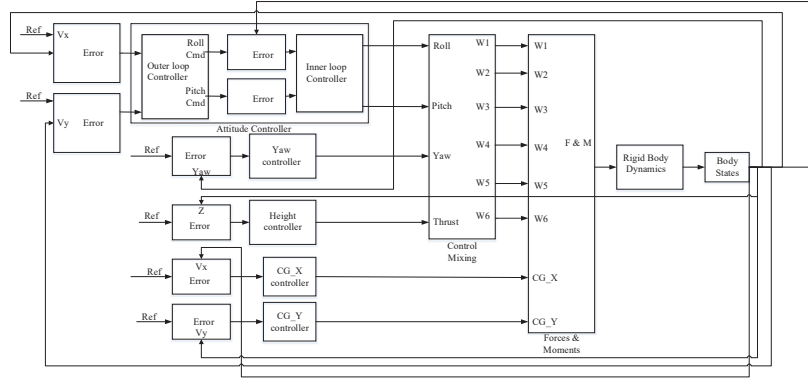


Figure 2. Top-level diagram of the over-actuated simulated Hexacopter plant



Figure 3. Airframe components and basic structure of the Hexacopter developed at UAV Laboratory of UNSW@ADFA

extremely difficult, where insertion of uncertainties and unknown disturbance is more challenging, or impossible in some cases. Thus, a controller that performs accurately with a minimum or no knowledge about the system is much needed in dealing with such autonomous vehicles. Being model-free and self-evolving data-driven, our developed G-controller is an appropriate candidate. Besides, the computational cost of our proposed controller is very low, where it maintains better tracking performance. The self-evolving architecture of our proposed G-controller is elaborated in the next section.

### III. ARCHITECTURE OF THE SELF-EVOLVING G-CONTROLLER

The self organizing mechanism of the G-controller is adopted from GENEFIS developed in [24]. GENEFIS is a TS FLS that features multidimensional membership functions in the input space where the contours are ellipsoid in arbitrary positions. Each estimated one dimensional membership functions represent a portion in the input space partition by assigning the Gaussian function's own center and width. Concurrently, our GENEFIS based G-controller is generating 1st order first-order polynomials as consequent parts of the fuzzy rules. In G-controller, a typical fuzzy rule can be expressed as follows:

$$\text{IF } Z \text{ is } R_i, \text{ then } \eta_i = a_{0i} + a_{1i}\zeta_1 + a_{2i}\zeta_2 + \dots + a_{ki}\zeta_k \quad (9)$$

where  $R_i$  represents the  $i$ -th rule (membership function) constructed from a concatenation of fuzzy sets and epitomizing a multidimensional kernel,  $k$  denotes the dimension of input feature,  $Z$  is an input vector of interest,  $a_i$  is the consequent parameter,  $\zeta_k$  is the  $k$ -th input feature. The predicted output of the self-evolving model can be expressed as:

$$\hat{\eta} = \sum_{i=1}^j \psi_i(\zeta) \eta_i(\zeta) = \frac{\sum_{i=1}^j R_i \eta_i}{\sum_{i=1}^j R_i} = \frac{\sum_{i=1}^j \exp(-(Z - \Theta_i) \Sigma_i^{-1} (Z - \Theta_i)^T) \eta_i}{\sum_{i=1}^j \exp(-(Z - \Theta_i) \Sigma_i^{-1} (Z - \Theta_i)^T)} \quad (10)$$

In Eq. 10,  $\Theta_i$  is the centroid of the  $i$ -th fuzzy rule  $\Theta_i \in \mathbb{R}^{1 \times j}$ ,  $\Sigma_i$  is a non-diagonal covariance matrix  $\Sigma_i \in \mathbb{R}^{k \times k}$  whose diagonal components are expressing the spread of the multivariate Gaussian function, and  $k$  is the number of fuzzy rules.

#### A. Statistical Contribution Based Rule Growing Mechanism

The Datum Significance (DS) method developed in [51] is utilized as a rule growing mechanism in G-controller. In our work, the original DS method is geared into the multivariate Gaussian membership function and polynomial consequents, which is the crux of GENEFIS [24]. The integration of the multivariate Gaussian membership function into the original DS method can be observed in our work as follows:

$$D_{sgn} = |e_{rn}| \int_Z \exp\left(-\frac{(Z - Z_n) \Sigma^{-1} (Z - Z_n)^T}{(Z - \Theta) \Sigma^{-1} (Z - \Theta)^T}\right) \frac{1}{\mathcal{H}(Z)} dz \quad (11)$$

where  $D_{sgn}$  denotes the the significance of the  $n$ -th datum,  $Z_n$  is the current input to the controller in a closed-loop control system  $Z_n \in \mathbb{R}$ , and  $\mathcal{H}(Z)$  is the range of input  $Z$ . In a closed-loop control system, error ( $e$ ) indicates the difference the desired reference and plant's output, which is usually fed as input to the controller. Whereas, error  $e_{rn}$  mentioned in Eq. 11 is difference from the input error ( $e$ ). The error  $e_{rn}$  can be expressed as:

$$|e_{rn}| = |tr_n - \eta_n| \quad (12)$$

where  $tr_n$  is the target, which is plant's output in our proposed G-controller, and  $\eta_n$  is control output from the G-controller at  $n$ -th episode. After applying  $k$ -fold numerical integration to Eq. 11, the following is obtained:

$$D_{sgn} = |e_{rn}| \left( \frac{\det(\Sigma_{j+1})}{\mathcal{H}(Z)} \right)^k \quad (13)$$

When the statistical contribution of the datum is higher the existing rules it becomes an appropriate candidate to be a new rule. Therefore, the DS criterion can be amended mathematically as follows:

$$D_{sgn} = |e_{rn}| \frac{\det(\Sigma_{j+1})^k}{\sum_{i=1}^{j+1} \det(\Sigma_i)^k} \quad (14)$$

When a sample lies far away from the nearest rule, a high value of  $D_{sgn}$  may obtain from Eq. 14 even with a small value of  $e_{rn}$ . In such situation, generalisation capability of the self-evolving neuro-fuzzy controller remains good without the addition of any new rules. Therefore, a high value of  $D_{sgn}$  does not always indicate the necessity of a rule evolution. On the other hand, a high value of  $e_{rn}$  may obtain in case of an overfitting phenomenon. In such case, the addition of a new rule may worsen the overfitting phenomenon. Thus, a separation is needed in Eq. 14 to cover two above mentioned discernible situation.

To overcome an overfitting scenario, it is important to monitor the effect of a newly injected sample on  $e_{rn}$ , since the structural learning is not occurring in every observation. In other words, the rule growing mechanism is probably turned on when the rate of change of  $e_{rn}$  is positive. In this work, the mean and variance of  $e_{rn}$  is measured by recursively updating  $e_{rn}$  and standard deviation [52] as follows:

$$\bar{e}_{rn} = \frac{n-1}{n} \bar{e}_{rn-1} + \frac{1}{n} e_{rn} \quad (15)$$

$$\bar{\sigma}_{rn}^2 = \frac{n-1}{n} \bar{\sigma}_{rn-1}^2 + \frac{1}{n} (e_{rn} - \bar{e}_{rn-1})^2 \quad (16)$$

When  $\bar{e}_{rn} + \bar{\sigma}_{rn}^2 - (\bar{e}_{rn-1} + \bar{\sigma}_{rn-1}^2) > 0$ , the DS criterion is simplified in our work as follows:

$$D_{sgn} = \frac{\det(\Sigma_{j+1})^k}{\sum_{i=1}^{j+1} \det(\Sigma_i)^k} \quad (17)$$

The condition in expanding the rule base utilizing Eq. 17 is  $D_{sgn} \geq g$ , where  $g$  is a predefined threshold. Eq. 17 represents an encouraging generalization and summarization of the datum, since a new rule can omit possible overfitting effects. Besides, this DS criterion can predict the probable contribution of the datum during its lifetime.

## B. Statistical Contribution Based Rule Pruning Mechanism

The Extended Rule significance (ERS) method was put forward by [51]. The ERS concept appraises the statistical contribution of the fuzzy rules when the number of observations is approaching infinity. The default ERS theory is not possible to integrate directly into GENEFIS's learning platform due to the incompatibility of default ERS concept with the NN. Numerous modifications are made in ERS theory to fit them with GENEFIS based G-controller. In this work, the concept of statistical contribution of the fuzzy rules can be expressed mathematically as follows:

$$\mathcal{E}(i, n) = |\delta_i| \mathcal{E}_i, \text{ where } |\delta_i| = \sum_{i=1}^{k+1} |\eta_i| \quad (18)$$

$$\mathcal{E}_i = \int_Z \exp(-(Z - \Theta_i^n) \Sigma_i^{-1} (Z - \Theta_i^n)^T) \frac{1}{\mathcal{H}(Z)} dz \quad (19)$$

From Eq. 18, it can be anticipated that the contribution of the fuzzy rules is a summary of the total contribution of input and output parts of the fuzzy rules, where  $\mathcal{E}_i$  is expressing the modified version of original input contribution explained in [51], [53], and  $\delta_i$  is explicating the contribution of output parameters. Usually, inverse covariance matrix  $\Sigma_i^{-1}$  in Eq. 19 has a smaller size than that of  $Z$ , which necessitates an amendment in Eq. 19 as follows:

$$\mathcal{E}_i \approx \frac{1}{\mathcal{H}(Z)} \left( 2 \int_0^\infty \exp\left(-\left(\frac{Z^2}{\det(\Sigma_i)}\right)\right) dz \right)^k \quad (20)$$

By using the  $k$ -fold numerical integration, the final version of ERS theory can be expressed as:

$$\mathcal{E}_{inf}^i = \sum_{i=1}^{j+1} \eta_i \frac{\det(\Sigma_i)^k}{\sum_{i=1}^j \det(\Sigma_i)^k} \quad (21)$$

When  $\mathcal{E}_{inf}^i \leq k_e$ , it is presumed that the clusters cannot capture the latest incoming data to the G-controller in the closed-loop control cycle. It can be deduced that the hyper-volume of the triggered cluster indicates the significance of the fuzzy rule. Thus, when the volume of the  $i$ th cluster is much lower than the summation of volumes of all cluster, that rule is considered as inconsequential. Such a rule is pruned to protect the rule base evolution from its adverse effect. In this work,  $k_e$  exhibits a plausible trade-off between compactness and generalization of the rule base. The allocated value for  $\delta$  is  $\delta = [0.0001, 1]$ , and  $k_e = 10\%$  of  $\delta$ .

## C. Adaptation of Rule Premise Parameters

Generalized Adaptive Resonance Theory+ (GART+) [54] is used in G-controller as a technique of granulating input features and adapting premise parameters. It is observed that GART [55] and its successor improved GART (IGART) [56] suffer from a category growing problem. In GRAT the compatibility measure is done utilizing the maximal membership degree of a new datum to all available rules. In first round if the selected category expresses a higher membership degree than a predefined threshold  $\rho_a$ , then it is declared as winning category



and the match tracking mechanism is executed. However, the first round winning category fails to beat the match tracking threshold  $\rho_b$ , which deactivates that category and increases the value of threshold  $\rho_a$  to find a better candidate. A larger width is required in the next selected category to cope with the increased value of  $\rho_a$ . Otherwise, it fabricates a new category. Nonetheless, a category with larger radii may contain more than one distinguishable data clouds and thereby marginalizing the other clusters in every training episode. In incremental learning environment this effect is known as *cluster delamination* [57], pictorially exhibited in Fig. 4. To relieve from the *cluster delamination* effect, in GENEFIS based G-controller the size of fuzzy rule are constrained by using GART+, which allows a limited grow or shrink of a category.

1) *Improved Selection procedure of winning Category*: To determine the most compatible or winning category Bayes's decision theory is utilized in GART+ [54]. To stimulate a more appropriate selection of the winning category, the Bayesian concept does not only consider the proximity of a category to the inserted datum, but also the dominance of the category with respect to the other categories through the category prior probability. That is, the category prior probability can count the number of samples falling in the outreach of the category, and is expressed as follows:

$$\hat{P}_r(\psi_i) = \frac{N_i}{\sum_{i=1}^j N_i} \quad (22)$$

where  $N_i$  indicates the number of times that  $i$ th category or fuzzy rule wins the competition.

When a new input datum to the controller finds two categories with almost similar distance but with different population number, Bayes's decision theory assists to select the category with more data points and declared it as a winning category. In the proposed G-controller, posterior probability of the  $i$ th category can be represented as follows:

$$\hat{P}_r(\psi_i|Z) = \frac{\hat{p}_r(Z|\psi_i)\hat{P}_r(\psi_i)}{\sum_{i=1}^j \hat{p}_r(Z|\psi_i)\hat{P}_r(\psi_i)} \quad (23)$$

where  $\hat{p}_r(\psi_i|Z)$  and  $\hat{P}_r(\psi_i)$  represents the likelihood and the prior probability correspondingly. The likelihood can also be elaborated as follows:

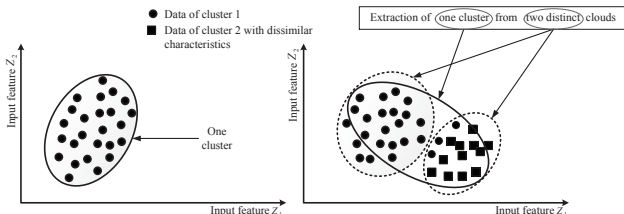


Figure 4. Cluster delamination effect (adapted from [24] with proper permission)

$$\hat{p}_r(Z|\psi_i) = \frac{1}{(2\pi V_i)^{1/2}} \exp(-(Z - \Theta_i)\Sigma_i^{-1}(Z - \Theta_i)^T) \quad (24)$$

where  $V_i$  determines the estimated hyper-volume of feature space covered by the  $i$ th category, which can be expressed as:

$$V_i = \det(\Sigma_i) \quad (25)$$

The Bayesian concept presented in Eq. 23 is implemented in G-controller, which can be interpreted as follows:

- 1) When a new sample is adjacent to existing categories, it causes a higher likelihood expressed by Eq. 24.
- 2) A category with a large volume is forced to divide its volume in Eq. 24, as a consequent it delivers a lower value of the posterior probability 23. This is important particularly to avoid large span clusters and to decrease the likelihood of cluster delamination effects.
- 3) According to 22, categories surrounded by more incoming data samples are more worthwhile, which inflicts a high value of posterior probability.

2) *Vigilance Test*: There are two goals to perform the vigilance test. The first goal concerns about the capability of the winning category to accommodate a new datum. The second goal is to reduce the size of the category, where a rule is not allowed to have a volume higher than the threshold  $V_{max}$ , that is calculated from  $V_{max} \equiv \rho_b \sum_{i=1}^j V_i$ . The vigilance test is a way to rule deletion, update, or evolution where it needs to be satisfied four different conditions as presented below:

$$\text{Case I: } R_{win} \geq \rho_a, V_{win} \leq V_{max} \quad (26)$$

where  $R_{win}$  is the membership degree of the winning rule to seize the latest datum. More importantly, the condition in Eq. 26 is indicating the capability of the selected category to accommodate the newest datum and emphasizing on the limited size of a category. In our proposed G-controller  $\rho_a$  is set close to 1. Contrarily, the value of  $\rho_b$  is set as [0.0001, 0.1]. Then the adaptation mechanism of focal point  $\Theta_i$ , and the dispersion matrix  $\Sigma_i$  is generated by the equations as follows:

$$\Theta_{win}^{new} = \frac{N_{win}^{old}}{N_{win}^{old} + 1} \Theta_{win}^{old} + \frac{(Z - \Theta_{win}^{old})}{N_{win}^{old} + 1} \quad (27)$$

$$\Sigma_{win}^{new-1} = \frac{\Sigma_{win}^{old-1}}{1 - \alpha} + \frac{\alpha}{1 - \alpha} \frac{\left( \Sigma_{win}^{old-1} (Z - \Theta_{win}^{new}) \right) \left( \Sigma_{win}^{old-1} (Z - \Theta_{win}^{new}) \right)^T}{1 + \alpha (Z - \Theta_{win}^{new}) \Sigma_{win}^{old-1} (Z - \Theta_{win}^{new})^T} \quad (28)$$

$$N_{win}^{new} = N_{win}^{old} + 1 \quad (29)$$

where  $\alpha$  can be expressed as follows:

$$\alpha = \frac{1}{N_{win}^{old} + 1} \quad (30)$$

where  $N_{win}^{old}$  denotes the number of training samples populating the winning cluster.

Besides, a major advantage of utilizing Eq. 28 is the prompter update of the dispersion matrix (inverse covariance



matrix), since a direct adjustment of the dispersion matrix is occurring without the necessity to re-inverse the dispersion matrix [58]. Concerning the conditions in 26, some pertinent likelihoods may emerge in the rehearsal process and they are outlined as follows:

Case II:  $R_{win} < \rho_a$ ,  $V_{win} > V_{max}$

In this circumstance, the input data to the G-controller cannot be touched by any existing rules of the controller, since the inserted input data is hardly covered by any rules. The statistical contribution of the datum needs to be calculated by DS-criterion. When both conditions are satisfied, a new rule is generated and its parameters are assigned as follows:

$$\Theta_{j+1} = Z \quad (31)$$

$$\text{diag}\left(\Sigma_{j+1}\right) = \frac{\max((\Theta_i - \Theta_{i-1}), (\Theta_i - \Theta_{i+1}))}{\sqrt{\frac{1}{\ln(\epsilon)}}} \quad (32)$$

where the value of  $\epsilon$  is 0.5. Equation 32 ensures a sufficient coverage of the newly added rule, which is proved in [59]. It helps GENEFIS to explore untouched regions in the feature space fitting a superfluous cluster at whatever point a relatively unexploited region or knowledge is fed, which is a mandatory element to confronting possible non-stationary and evolving qualities of the self-evolving control system. Note that proper initialization of inverse covariance matrix plays a crucial role to the success of multivariate Gaussian fuzzy rule. Although it meets the  $\epsilon$ -completeness criterion, Equation 32 requires re-inversion phase which sometimes leads to instability when the covariance matrix is not full-rank. As an alternative, the inverse covariance matrix can be initialized as:

$$\Sigma_0^{-1} = k_{fs}I \quad (33)$$

where  $k_{fs}$  is a user-defined parameter, and  $I$  is an identity matrix.

Case III:  $R_{win} \geq \rho_a$ ,  $V_{win} > V_{max}$

This situation is indicating the capability of existing rule base to cover the current data easily. However, the width of the chosen cluster is oversized. This datum creates a redundancy when added to the rule base. To mitigate the adverse impact, one of the solutions is to replace the selected cluster merely by this datum. Then the fuzzy region is eased as follows:

$$\Theta_{win} = Z \quad (34)$$

$$\Sigma_{win}^{new-1} = \frac{1}{k_{win}} \Sigma_{win}^{old-1} \quad (35)$$

where  $k_{win}$  is a constant with a value of 1.1, and the width of the cluster is reduced until a desirable fuzzy region is obtained while satisfying  $V_{win} \leq V_{max}$ .

Case IV:  $R_{win} < \rho_a$ ,  $V_{win} \leq V_{max}$

The same action is taken as in Case I, i.e., the adjustment process is executed to stimulate the category to move towards the incoming input data.

#### IV. SMC THEORY-BASED ADAPTATION OF G-CONTROLLER

In our work, an advanced self-evolving neuro-fuzzy system called GENEFIS is utilized to build the evolving structure

and adapt premise parameters of the proposed G-controller, where the integration of multivariate Gaussian function and GART+ method helps the controller to reduce the structural complexity and to adapt with sharp changes in autonomous vehicle's plant dynamics. On the other hand, being robust enough to guarantee the robustness of a system against external perturbations, parameter variations, unknown uncertainties, the SMC theory is applied in our work to adapt the consequent parameters of the G-controller. In SMC scheme, the motion of a system is restricted to a plane known as *sliding surface*. In this work, the SMC learning theory-based adaptation laws are developed to establish a stable closed-loop system. By following the regulations of SMC scheme as explained in [60], [61], [62], the zero dynamics of the learning error coordinate is defined as time-varying sliding surface as follows:

$$S_{ssr}(u_g, u) = u_{ARC}(t) = u_g(t) + u(t) \quad (36)$$

The sliding surface for the highly nonlinear over-actuated autonomous vehicles namely FW MAV, and hexacopter plant to be controlled is expressed as:

$$s_H = e + \lambda_1 \dot{e} + \lambda_2 \int_0^t e(\tau) d\tau \quad (37)$$

where,  $\lambda_1 = \frac{\alpha_2}{\alpha_1}$ ,  $\lambda_2 = \frac{\alpha_3}{\alpha_1}$ ,  $e$  is the error which is the difference between the actual displacement from the plant and desired position in case of altitude control. In this work, in case the BIFW MAV plant, the sliding parameter  $\alpha_1$  has initialized with a small value  $1 \times 10^{-2}$ , whereas  $\alpha_2$  has initialized with  $1 \times 10^{-3}$ , and  $\alpha_3 \approx 0$ . Each of the parameters is then evolved by using learning rates. These learning rates are set in such a way so that the sliding parameters can achieve the desired value in the shortest possible time to create a stable closed-loop control system. A higher initial value of the sliding parameters is avoided, since it may cause a big overshoot at the beginning of the trajectory. It can be abstracted that, to make our proposed G-controller absolutely model free, these sliding parameters are self-organizing rather than predefined constant values.

*Definition* : After a certain time  $t_k$  a sliding motion will be developed on the sliding manifold  $S_{ssr}(u_g, u) = u_{ARC}(t) = 0$ , where the state  $S_{ssr}(t)\dot{S}_{ssr}(t) = u_{ARC}(t)\dot{u}_{ARC}(t) < 0$  to be satisfied for the whole time period with some nontrivial semi-open sub-interval of time expressed as  $[t, t_k) \subset (0, t_k)$ .

It is expected to produce such online adaptation of consequent parameters of the proposed G-controller that the sliding mode condition of the aforesaid definition is enforced. The adaptation process of the proposed method is summarized below.

**Theorem 1.** *The adaptation laws for the consequent parameters of the G-controller are chosen as:*

$$\dot{\omega}(t) = -\alpha_1 G(t)\psi(t)s_H(t), \quad \text{where } \omega(0) = \omega_0 \in \mathfrak{R}^{nR \times 1} \quad (38)$$

where the term  $G(t)$  can be updated recursively as follows:

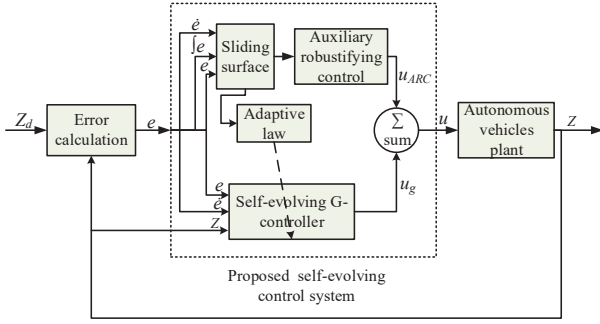


Figure 5. Self-evolving G-controller based closed-loop control system

$$\dot{G}(t) = -G(t)\psi(t)\psi^T(t)G(t), \quad \text{where } G(0) = G_0 \in \mathfrak{R}^{nR \times nR} \quad (39)$$

where  $n$  is the number of inputs to the controller, and  $R$  is the number of generated rules. These adaptation laws guarantee a stable closed-loop control system, where the plants to be controlled can be of various order.

*Proof* : The sliding parameter dependent robustifying auxiliary control term of the proposed controller can be expressed as follows:

$$u_{ARC}(t) = \alpha_1 s_H \quad (40)$$

The robustifying auxiliary control term  $u_{ARC}$  may suffer from high-frequency oscillations in the control input. It is an undesirable phenomenon in sliding mode controller and known as chattering effect. Due to simplicity, saturation or sigmoid functions are mostly used to reduce the chattering effect. In this work, a saturation function is utilized to mitigate the adverse effect of chattering.

The G-controller's final output signal can be expressed as follows:

$$u_g(t) = \psi^T(t)\omega(t) \quad (41)$$

The overall control signal as observed in Fig.(5) can be obtained as follows:

$$u(t) = u_{ARC}(t) - u_g(t) \quad (42)$$

The cost function can be defined as:

$$\begin{aligned} J(t) &= \int_0^t s_H^2(\tau) d\tau \\ &= \frac{1}{\alpha_1^2} \int_0^t (u(\tau) + u_g(\tau))^2 d\tau \\ &= \frac{1}{\alpha_1^2} \int_0^t (u(\tau) + \psi^T(t)\omega(\tau))^2 d\tau \end{aligned} \quad (43)$$

The gradient of  $J$  with respect to  $\omega$  is as follows:

$$\begin{aligned} \nabla_{\omega} J(t) &= 0 \\ \Rightarrow \int \psi(\tau)u(\tau) d\tau + \omega(t) \int_0^t \psi(\tau)\psi^T(\tau) d\tau &= 0 \\ \Rightarrow \omega(t) &= \left[ \int_0^t \psi(\tau)\psi^T(\tau) d\tau \right]^{-1} \int_0^t \psi(\tau)u(\tau) d\tau \quad (44) \\ \Rightarrow \omega(t) &= -G(t) \int_0^t \psi(\tau)u(\tau) d\tau \quad (45) \\ \Rightarrow G^{-1}(t)\omega(t) &= - \int_0^t \psi(\tau)u(\tau) d\tau \quad (46) \end{aligned}$$

where,

$$G(t) = \left[ \int_0^t \psi(\tau)\psi^T(\tau) d\tau \right]^{-1} \quad (47)$$

$$G^{-1}(t) = \int_0^t \psi(\tau)\psi^T(\tau) d\tau \quad (48)$$

The derivative of Eq. (48) is as follows:

$$\begin{aligned} G^{-1}(t)\dot{G}(t)G^{-1}(t) &= -\psi(t)\psi^T(t) \\ \dot{G}(t) &= -G(t)\psi(t)\psi^T(t)G(t) \end{aligned} \quad (49)$$

From Eq. (49), it is observed that  $\dot{G}(t)$  is a negative definite and  $G(t)$  is decreasing over time, therefore  $G(t) \in l_{\infty}$ . Now executing the time derivative of Eq. (45) and utilizing Eq. Fig. 6(a)(40), (41), (42), and (46) the following is obtained:

$$\begin{aligned} \dot{\omega}(t) &= \dot{G}(t)G^{-1}(t)\omega(t) - G(t)\psi(t)u(t) \\ &= -G(t)\psi(t)\psi^T(t)\psi(t)\omega(t) - G(t)\psi(t)u(t) \\ &= -G(t)\psi(t) (\psi^T(t)\omega(t) + u(t)) \\ &= -\alpha_1 G(t)\psi(t)s_H(t) \end{aligned} \quad (50)$$

1) *Stability Analysis: Definition* : FLS is known as a general function approximator. Therefore, in this work it is assumed that without loss of generality there exists a  $\omega^*$  such that:

$$u(t) = \psi^T \omega^*(t) + \varepsilon_f^*(z) \quad (51)$$

where  $\varepsilon_f^*(z) = [\varepsilon_{f1}^*, \varepsilon_{f1}^*, \dots, \varepsilon_{f1}^*]^T \in \mathfrak{R}^k$  is the minimal functional approximator error. In this work, the following is defined:

$$\tilde{\omega}(t) = \omega(t) - \omega^* \quad (52)$$

In addition:

$$s_H(t) = \psi^T \tilde{\omega}(t) \quad (53)$$

*Lemma 1* :

$$\begin{aligned} \frac{d(G^{-1}(t)\tilde{\omega}(t))}{dt} &= -G^{-1}(t)\dot{G}(t)G^{-1}(t)\tilde{\omega}(t) + G^{-1}(t)\dot{\tilde{\omega}}(t) \\ &= \psi(t)\psi^T(t)\tilde{\omega}(t) - \psi(t)s_H(t) \\ &= \psi(t)s_H(t) - \psi(t)s_H(t) \\ &= 0 \end{aligned} \quad (54)$$

This is indicating that  $G^{-1}(t)\tilde{\omega}(t)$  is not altering with respect to time, and therefore  $G^{-1}(t)\tilde{\omega}(t) = G^{-1}(0)\tilde{\omega}(0)$ ,  $\forall t > 0$ .

$$\lim_{t \rightarrow \infty} \tilde{\omega}(t) = \lim_{t \rightarrow \infty} G(t)G^{-1}(0)\tilde{\omega}(0) \quad (55)$$

Since  $G(t)$  is decreasing and  $\tilde{\omega}(t) \in l_\infty, \omega(t) \in l_\infty$ . In this work the following Lyapunov function is considered:

$$V(t) = \frac{1}{2}\tilde{\omega}^T(t)G^{-1}(t)\tilde{\omega}(t) \quad (56)$$

The time derivative of the Lyapunov function is as follows:

$$\begin{aligned} \dot{V}(t) &= \frac{1}{2}\tilde{\omega}^T(t)G^{-1}\dot{\tilde{\omega}}(t) + \frac{1}{2}\tilde{\omega}^T(t)\dot{G}^{-1}\tilde{\omega}(t) \\ &= -\tilde{\omega}^T(t)\psi(t)s_H(t) - \frac{1}{2}\tilde{\omega}^T(t)\psi(t)\psi^T(t)\tilde{\omega}(t) \\ &= -s_H^2(t) - \frac{1}{2}s_H^2(t) \\ &= -\frac{3}{2}s_H^2(t) \leq 0 \end{aligned} \quad (57)$$

From Eq. 56, and Eq. 57, it is observed that  $V(t) > 0$ , and  $\dot{V}(t) \leq 0$ . In addition, Eq. 57 shows that  $\dot{V}(t) = 0$ , if and only if  $e(t) = 0$ . It is indicating that the global stability of the system is guaranteed by the Lyapunov theorem. By utilizing Barbalat's lemma [63], it can also be observed that  $e(t) \rightarrow 0$  as  $t \rightarrow \infty$ . It is ensuring the asymptotic stability of the system. Thus, a convergence of the system's tracking error to zero is witnessed.

## V. RESULTS AND DISCUSSION

In this work, the self-evolving generic neuro-fuzzy controller namely G-controller is attempted to control of autonomous vehicles online. As mentioned in Section II that the G-controller is utilized in controlling a BIFW MAV and a hexacopter UAV. In case of the BIFW MAV, various altitude trajectory tracking is observed to evaluate the controller's performance, whereas, in hexacopter, not only the altitude but also the attitude tracking is witnessed. Being an evolving controller, the G-controller can evolve both the structure and parameters. The observed evaluation procedure from the G-controller's performance is explained in the following subsection V-A.

### A. Evaluation Procedure

The proposed G-controller has the capability of evolving the structure by adding or pruning the rules like many other evolving controllers discussed in the subsection I-A. However, unlike the existing evolving controller, GRAT+, multivariate Gaussian function, SMC learning theory based adaptation laws are combined in the G-controller. From the amalgamation of such advanced features, the faster self-evolving mechanism is recorded with a lower computational cost. In controlling the altitude and attitude of the highly nonlinear and complex autonomous vehicles discussed in Section II, the activation of only the rule growing mechanism was sufficient. Due to the evolving nature of the G-controller, the fuzzy rules are generated in different time steps for different reference

signals. This rule generation of the G-controller with respect to various desired altitude of BIFW MAV are compiled in a table provided in the supplementary document. To understand graphically, the number of generated rules for various trajectories of BIFW MAV and Hexacopter are plotted and disclosed in Fig. 12.

### B. Results

The G-controller's performance is observed with respect to various reference signals, and the results are compared with a TS fuzzy controller [64], and a Proportional Integral Derivative (PID) controller. Our source codes are made publicly available in [25]. In case of the BIFW MAV, variety of desired trajectories were utilized in the closed-loop control system to evaluate controllers performance for 100 seconds, such as: 1) a constant altitude of 10 meters expressed as  $Z_d(t) = 10$ ; 2) three different step functions, where one of them is varying its amplitude from 0 m to 10 m, another is from 5 m to 10 m, and the other one is varying from -5 m to 5m, presented as  $Z_d(t) = 10u(t - 20)$ ,  $Z_d(t) = 5u(t) + 5u(t - 20)$ ,  $Z_d(t) = -5u(t) + 10u(t - 20)$  respectively; 3) three different square wave function with a frequency of 0.1 Hz, and amplitude of 1 m, 4 m, and 10 m correspondingly; 4) two square wave function with a frequency of 1 Hz, and amplitude of 1 m and 4 m; 5) a customized trajectory, where the amplitude varies from 0 to 2 m; 6) a sawtooth wave function with an amplitude of 1 m and frequency of 1 Hz; 7) a sine wave function with an amplitude of 1 m and frequency of 1 Hz. For all these trajectories, the performance of our proposed G-controller, TS fuzzy controller, and PID controller is observed and compared, where higher accuracy is obtained from the G-controller. For clearer understanding, some of these observations are presented pictorially from Fig. 6 to Fig. 9.

The performance of various controllers for a step function  $Z_d(t) = 5u(t) + 5u(t - 20)$  is observed in Fig. 6, where our proposed G-controller outperformed the PID, and TS fuzzy controller. The performance of the trajectory like square wave pulse with an amplitude of 4 m and frequency of 1 Hz is observed in Fig. 7, where comparatively improved performance is witnessed from our developed G-controller. In case of this trajectory the TS fuzzy controller fails to follow the trajectory. Therefore, the comparison only between the PID and G-controller is exposed in Fig. 7, where the G-controller has beaten the PID controller in terms of accuracy. In case of all the trajectories for BIFW MAV exposed in this paragraph, superior performance is visualized by our proposed G-controller. To observe the controllers performance deeply, the root mean square error (RMSE), rising time, and settling time of all the controllers for various reference signals are measured and summarized in TABLE II, where the lowest RMSE is inspected from the G-controller. Since the G-controller starts operating from scratch with an empty fuzzy set, the rising time is comparatively higher than the PID controller. However, comparatively lower settling time is indicating the proposed controllers ability to back to the desired trajectory sharply.

A wind gust is added to the BIFW MAV plant dynamics to check the robustness of our proposed G-controller against

unknown perturbations and uncertainties. This simulated wind gust has a maximum velocity of  $40 \text{ m s}^{-1}$  and is applied to the plant after 2 seconds. In the presence of the wind gust, some of the trajectory tracking performances of the controllers are manifested in Fig. 9, where an insignificant deterioration in tracking is observed at the beginning. However, this adverse effect has been minimized very sharply by the G-controller. The RMSE by considering the effect of wind gust are also tabulated in TABLE II.

Furthermore, the G-controller has been utilized to control altitude, the outer loop of attitude (roll and pitch) of the simulated over-actuated hexacopter plant developed in ADFA and results are compared with a PID controller. In case of controlling the altitude, the controllers are employed to control the thrust of the control-mixing box of the plant. Due to the addition of the moving mass, the rolling motion is not only controlled by the velocity in Y-axis ( $v_y$ ) generated by the motors, but also the mass moving in the Y direction due to their Center of Gravity (CG) shifting capability. Our proposed controller has been employed in both facts to control the rolling motion. Similarly, to control the pitching motion of the hexacopter, the G-controller has been used to control both the velocity in X-axis ( $v_x$ ) and the mass moving in the X direction. The altitude tracking performance of hexacopter for various trajectories has been observed in Fig. 10, whereas the tracking of rolling and pitching is exhibited in Fig. 11. In all cases, better tracking has been monitored from the G-controller than that of PID controller. The RMSE, rise time, and settling time has been calculated for all the trajectories of the hexacopter and outlined in a TABLE provided in the supplementary document, where lower RMSE is perceived from the proposed G-controller. Besides, the settling time of the G-controller is much lower than that of the PIDs, which clearly indicates their improvement over the PID controller.

### C. Discussion

Unlike the PID and TS fuzzy controller, the G-controller starts the self-construction online with an empty fuzzy set at the beginning of the closed-loop control system. Whereas, the PID and TS fuzzy controller start operating with their pre-set control parameters. In case of the PID controller, control parameters (proportional gain  $K_p$ , integral gain  $K_i$ , and differential gain  $K_D$ ) are obtained offline before starting the closed-loop control operation. The TS fuzzy controller consists of five rules, where univariate Gaussian membership functions are utilized in each rule. To obtain the antecedents and consequent parameters of the rules, the fuzzy controller is trained with the PID controller's input and output datasets. It is clear that in both PID and TS fuzzy controllers the parameters are fixed before the starting of the closed-loop control system. On the contrary, in G-controller not only the GENEFIS but also the parameters of the sliding surface are evolving. Those sliding parameters are initialized with a very small value, then evolved to a desired value by using different learning rates. These rates are varied with respect to the corresponding plants, and desired actions. To the best of our knowledge, this approach of evolving the sliding parameters is never

utilized before in any of the existing evolving neuro-fuzzy controllers. It makes the proposed G-controller a fully self-evolving controller.

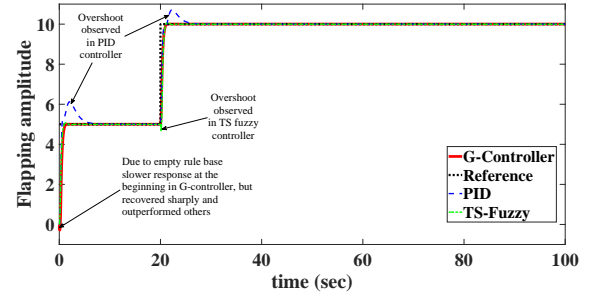


Figure 6. Performance observation of various controllers in altitude tracking of BIFW MAV when the trajectory is a step function  $Z_d(t) = 5u(t) + 5u(t-20)$

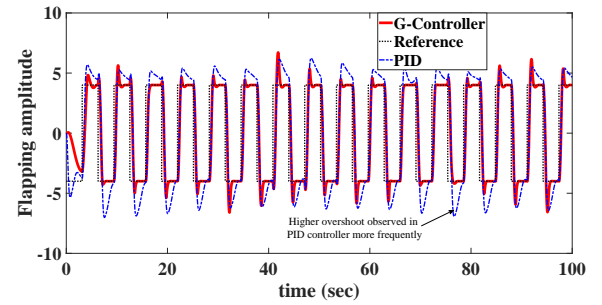


Figure 7. Performance observation of various controllers in altitude tracking of BIFW MAV when the trajectory is a square wave function with an amplitude of 4 m and frequency 1 Hz

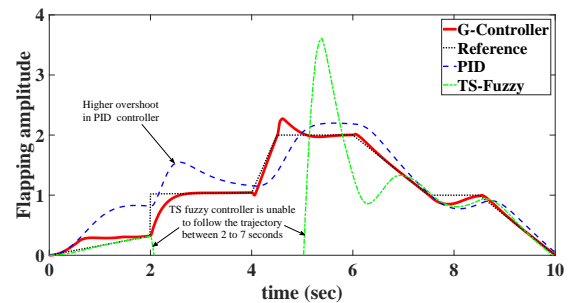


Figure 8. Performance observation of various controllers in BIFW MAV in case of tracking a customized trajectory

Table II  
MEASURED RMSE, RISE AND SETTLING TIME OF VARIOUS CONTROLLERS IN OPERATING THE BIFW MAV

Desired Trajectory ( $Z_d$ )	Maximum amplitude (meter)	Measured features	Without gust			With gust			
			PID	TS-Fuzzy	G-controller	PID	TS-Fuzzy	G-controller	
Constant height	10	RMSE	0.6630	<b>0.5693</b>	0.6460	0.6635	<b>0.5708</b>	0.6461	
		Rise time (sec)	0.9040	<b>0.7442</b>	1.2583	0.9040	<b>0.7442</b>	0.7984	
		Settling time (sec)	8.2595	4.9305	<b>3.9525</b>	10.1	3.6	<b>2.6</b>	
Step function	$Z_d(t) = 5u(t) + 5u(t - 20)$	RMSE	0.4000	0.4023	<b>0.3866</b>	0.3962	0.4002	<b>0.3865</b>	
		Rise time (sec)	21.242	<b>21.094</b>	21.37	21.23	<b>21.05</b>	21.12	
		Settling time (sec)	28.1	23.01	<b>21.50</b>	27.5	23.6	<b>21.80</b>	
	$Z_d(t) = 10u(t - 20)$	RMSE	0.6266	0.6701	<b>0.5677</b>	0.6216	0.6616	<b>0.5611</b>	
		Rise time (sec)	21.03	20.91	<b>20.746</b>	21.02	20.81	<b>20.75</b>	
		Settling time (sec)	29.50	<b>22.05</b>	22.07	32.02	24.99	<b>21.66</b>	
	$Z_d(t) = -5u(t) + 10u(t - 20)$	RMSE	0.6695	0.7188	<b>0.6535</b>	0.6648	0.7109	<b>0.6477</b>	
		Rise time (sec)	21.035	<b>20.95</b>	21.53	21.02	20.81	<b>20.79</b>	
		Settling time (sec)	29.5	22.5	<b>22.1</b>	31.56	24.59	<b>21.03</b>	
Square wave function ( $f = 0.1 Hz$ )	1	RMSE	0.2039	0.2493	<b>0.1746</b>	0.2020	0.2552	<b>0.1710</b>	
		Rise time (sec)	<b>0.38</b>	0.48	0.83	<b>63.18</b>	63.43	63.45	
		Settling time (sec)	10.11	3.8	<b>2.75</b>	69.52	69.50	<b>67.05</b>	
	4	RMSE	0.8909	0.9059	<b>0.8337</b>	0.8892	0.9025	<b>0.8311</b>	
		Rise time (sec)	<b>0.45</b>	0.524	0.914	<b>0.49</b>	0.52	0.91	
		Settling time (sec)	6.75	5.6	<b>2.5</b>	8.92	5.14	<b>2.15</b>	
	10	RMSE	2.7381	511.9071	<b>2.5406</b>	2.7339	1629.4883	<b>2.5376</b>	
		Rise time (sec)	<b>23.30</b>	N/A	23.37	<b>0.97</b>	N/A	1.26	
		Settling time (sec)	42.5	N/A	<b>34.5</b>	8.37	N/A	<b>2.25</b>	
Square wave function ( $f = 1 Hz$ )	1	RMSE	0.6719	362.9960	<b>0.5893</b>	0.6720	363.3044	<b>0.5735</b>	
		Rise time (sec)	<b>3.43</b>	N/A	3.72	<b>3.435</b>	N/A	4.17	
		Settling time (sec)	22.6	N/A	<b>8.5</b>	18.1	N/A	<b>4.4</b>	
	4	RMSE	3.1435	573.3459	<b>2.7275</b>	3.1336	1258.0926	<b>2.6766</b>	
		Rise time (sec)	<b>3.752</b>	N/A	4.06	<b>4.13</b>	N/A	4.62	
		Settling time (sec)	12.4	N/A	<b>7.81</b>	6.58	N/A	<b>4.74</b>	
	Customized wave function	2	RMSE	0.2856	4.7793	<b>0.1033</b>	0.2846	4.7708	<b>0.1026</b>
			Rise time (sec)	2.0	<b>1.30</b>	1.98	2.16	<b>0.93</b>	1.96
			Settling time (sec)	5.5	7.25	<b>2.8</b>	7.66	7.25	<b>2.75</b>
Sawtooth wave function	1	RMSE	0.5235	325.4397	<b>0.4781</b>	0.5240	325.4111	<b>0.4776</b>	
		Rise time (sec)	<b>0.24</b>	N/A	0.96	0.9039	N/A	<b>0.6499</b>	
		Settling time (sec)	4.1	N/A	<b>1.5</b>	5.68	N/A	<b>0.65</b>	
Sine wave function	1	RMSE	0.2096	0.0737	<b>0.0356</b>	0.1880	0.0764	<b>0.0395</b>	
		Rise time (sec)	<b>0.824</b>	1.19	1.01	<b>0.7405</b>	1.19	1.08	
		Settling time (sec)	4.1	3.4	<b>2.7</b>	5.23	3.32	<b>2.11</b>	

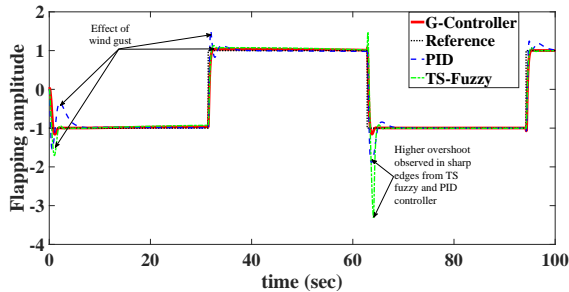


Figure 9. Performance observation of various controllers in altitude tracking of BIFW MAV by considering wind gust as environmental uncertainty

VI. CONCLUSIONS

The G-controller developed in this work is an entirely model-free approach and self-evolving in nature, i.e. it can alter its structure, and system parameters online to cope with changing dynamics of the plant to be controlled. Besides, the synthesis of SMC theory based adaptation laws improve its robustness against various internal and external uncertainties. These desirable features make the G-controller a suitable candidate for highly nonlinear autonomous vehicles. In this

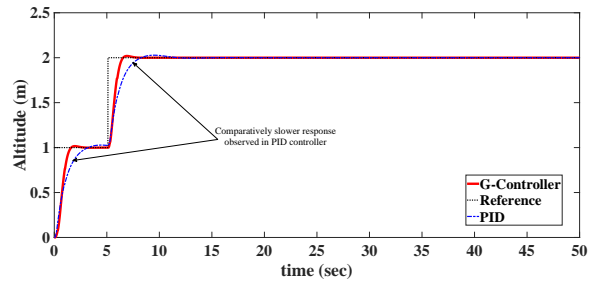


Figure 10. Performance observation of a PID and proposed G-controller in tracking various altitude of a hexacopter

work, our proposed control algorithm is developed using C programming language considering the compatibility issues to implement directly in hardware of a variety of autonomous vehicles like BIFW MAV, quadcopter, hexacopter, etc. The controller’s performance has been evaluated by observing the tracking performance of an over-actuated BIFW MAV and an over-actuated hexacopter’s plant with respect to a variety of trajectories. The performances are compared to that of a PID, and a TS fuzzy controller to observe the improvements in our proposed online evolving G-controller. The G-controller starts

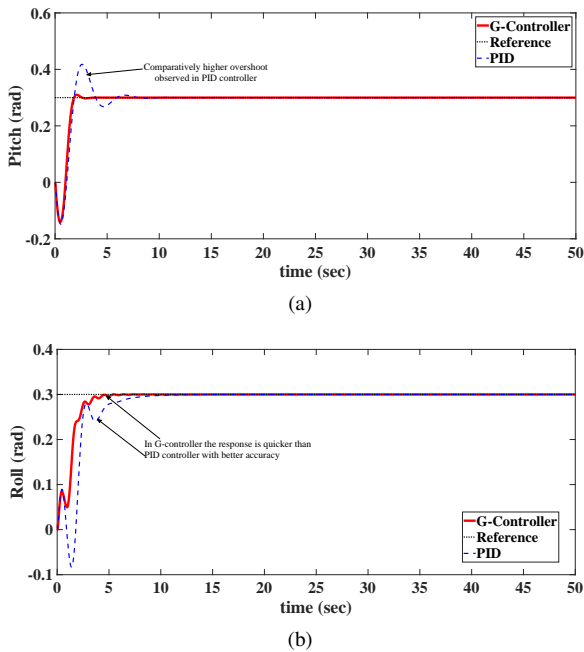


Figure 11. Performance observation of a PID and proposed G-controller in tracking desired (a) pitching and (b) rolling motion of a hexacopter

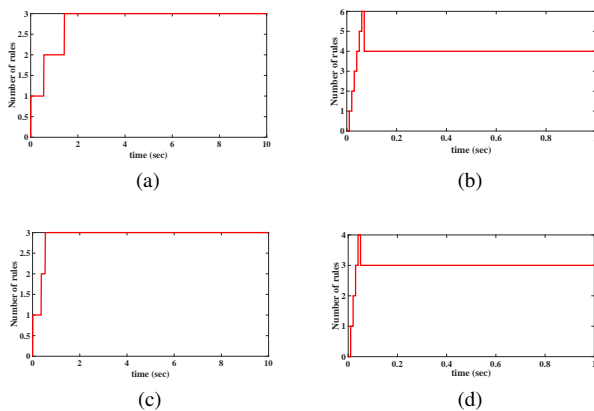


Figure 12. Generated rules of the self-evolving G-controller at various trajectories of BIFW MAV and hexacopter where the trajectories are (a) step function altitude for BIFW MAV, (b) customized altitude for BIFW MAV, (c) pitching for Hexacopter, (d) rolling for Hexacopter

building the structure from scratch with an empty fuzzy set in the closed-loop system. It causes a slow response at the very beginning of the loop, which is a common phenomenon in any self-evolving controller. However, due to the integration of GRAT+, multivariate Gaussian function, SMC learning theory based adaptation laws, the self-evolving mechanism of the G-controller is faster with a lower computational cost. In addition, wind gust has been added to the BIFW MAV plant as environmental uncertainties to evaluate the G-controller's robustness against unknown perturbations, where satisfactory tracking of the desired trajectory proves the proposed controller performance to eliminate various uncertainties. Thus, the G-controller's stability is confirmed by both the Lyapunov theory and experiments. In future, the controller will be executed through hardware-based flight test of various unmanned

aerial vehicles.

## ACKNOWLEDGEMENT

The authors would like to thank the Australian Defense Science and Technology Group for providing the simulated BIFW MAV plant, Unmanned Aerial Vehicle laboratory of the UNSW at the Australian Defense Force Academy for supporting with the hexacopter plants, and the computational support from the Computational Intelligence Laboratory of Nanyang Technological University (NTU) Singapore. This work is fully supported by NTU start-up grant and MOE tier-1 grant.

## REFERENCES

- [1] H. Gomi and M. Kawato, "Neural network control for a closed-loop system using feedback-error-learning," *Neural Networks*, vol. 6, no. 7, pp. 933–946, 1993.
- [2] Y.-J. Liu and S. Tong, "Adaptive fuzzy identification and control for a class of nonlinear pure-feedback mimo systems with unknown dead zones," *IEEE Transactions on Fuzzy Systems*, vol. 23, no. 5, pp. 1387–1398, 2015.
- [3] J. R. Noriega and H. Wang, "A direct adaptive neural-network control for unknown nonlinear systems and its application," *IEEE Transactions on Neural Networks*, vol. 9, no. 1, pp. 27–34, 1998.
- [4] T. Takagi and M. Sugeno, "Fuzzy identification of systems and its applications to modeling and control," in *Readings in Fuzzy Sets for Intelligent Systems*. Elsevier, 1993, pp. 387–403.
- [5] R.-J. Wai and P.-C. Chen, "Intelligent tracking control for robot manipulator including actuator dynamics via tsk-type fuzzy neural network," *IEEE Transactions on Fuzzy Systems*, vol. 12, no. 4, pp. 552–560, 2004.
- [6] S. L. Perić, D. S. Antić, M. B. Milovanović, D. B. Mitić, M. T. Milojković, and S. S. Nikolić, "Quasi-sliding mode control with orthogonal endocrine neural network-based estimator applied in anti-lock braking system," *IEEE/ASME Transactions on Mechatronics*, vol. 21, no. 2, pp. 754–764, 2016.
- [7] C.-J. Lin, "A ga-based neural fuzzy system for temperature control," *Fuzzy Sets and Systems*, vol. 143, no. 2, pp. 311–333, 2004.
- [8] F.-J. Lin, C.-H. Lin, and P.-H. Shen, "Self-constructing fuzzy neural network speed controller for permanent-magnet synchronous motor drive," *IEEE transactions on fuzzy systems*, vol. 9, no. 5, pp. 751–759, 2001.
- [9] R.-J. Wai and L.-C. Shih, "Adaptive fuzzy-neural-network design for voltage tracking control of a dc-dc boost converter," *IEEE transactions on power electronics*, vol. 27, no. 4, pp. 2104–2115, 2012.
- [10] Y. Pan, T. Sun, and H. Yu, "Peaking-free output-feedback adaptive neural control under a nonseparation principle," *IEEE transactions on neural networks and learning systems*, vol. 26, no. 12, pp. 3097–3108, 2015.
- [11] Y. Pan and H. Yu, "Biomimetic hybrid feedback feedforward neural-network learning control," *IEEE transactions on neural networks and learning systems*, vol. 28, no. 6, pp. 1481–1487, 2017.
- [12] Y. Pan, T. Sun, Y. Liu, and H. Yu, "Composite learning from adaptive backstepping neural network control," *Neural Networks*, vol. 95, pp. 134–142, 2017.
- [13] T. Sun, H. Pei, Y. Pan, H. Zhou, and C. Zhang, "Neural network-based sliding mode adaptive control for robot manipulators," *Neurocomputing*, vol. 74, no. 14, pp. 2377–2384, 2011.
- [14] M. Pratama, S. G. Anavatti, P. P. Angelov, and E. Lughofer, "Panfis: A novel incremental learning machine," *IEEE Transactions on Neural Networks and Learning Systems*, vol. 25, no. 1, pp. 55–68, 2014.
- [15] Y. Gao and M. J. Er, "Online adaptive fuzzy neural identification and control of a class of mimo nonlinear systems," *IEEE Transactions on Fuzzy Systems*, vol. 11, no. 4, pp. 462–477, 2003.
- [16] P. Angelov, "A fuzzy controller with evolving structure," *Information Sciences*, vol. 161, no. 1, pp. 21–35, 2004.
- [17] C.-M. Lin and T.-Y. Chen, "Self-organizing cmac control for a class of mimo uncertain nonlinear systems," *IEEE Transactions on Neural Networks*, vol. 20, no. 9, pp. 1377–1384, 2009.
- [18] J.-C. de Barros and A. L. Dexter, "Evolving fuzzy model-based adaptive control," in *Fuzzy Systems Conference, 2007. FUZZ-IEEE 2007. IEEE International*. IEEE, 2007, pp. 1–5.



- [19] I. Škrjanc, S. Blažič, and P. Angelov, "Robust evolving cloud-based pid control adjusted by gradient learning method," in *Evolving and Adaptive Intelligent Systems (EAIS), 2014 IEEE Conference on*. IEEE, 2014, pp. 1–8.
- [20] D. Leite, R. M. Palhares, V. C. Campos, and F. Gomide, "Evolving granular fuzzy model-based control of nonlinear dynamic systems," *IEEE Transactions on Fuzzy Systems*, vol. 23, no. 4, pp. 923–938, 2015.
- [21] H.-G. Han, X.-L. Wu, and J.-F. Qiao, "Real-time model predictive control using a self-organizing neural network," *IEEE Transactions on Neural Networks and Learning Systems*, vol. 24, no. 9, pp. 1425–1436, 2013.
- [22] H. Han and J. Qiao, "Nonlinear model-predictive control for industrial processes: An application to wastewater treatment process," *IEEE Transactions on Industrial Electronics*, vol. 61, no. 4, pp. 1970–1982, 2014.
- [23] H.-G. Han, L. Zhang, Y. Hou, and J.-F. Qiao, "Nonlinear model predictive control based on a self-organizing recurrent neural network," *IEEE Transactions on Neural Networks and Learning Systems*, vol. 27, no. 2, pp. 402–415, 2016.
- [24] M. Pratama, S. G. Anavatti, and E. Lughofer, "Genefis: toward an effective localist network," *IEEE Transactions on Fuzzy Systems*, vol. 22, no. 3, pp. 547–562, 2014.
- [25] M. M. Ferdous and M. Pratama, "G controller code," 2018. [Online]. Available: <https://www.ntu.edu.sg/home/mpratama/Publication.html>
- [26] M. Pratama, S. G. Anavatti, M. Garratt, and E. Lughofer, "Online identification of complex multi-input-multi-output system based on generic evolving neuro-fuzzy inference system," in *Evolving and Adaptive Intelligent Systems (EAIS), 2013 IEEE Conference on*. IEEE, 2013, pp. 106–113.
- [27] N. Wang, M. J. Er, J.-C. Sun, and Y.-C. Liu, "Adaptive robust online constructive fuzzy control of a complex surface vehicle system," *IEEE Transactions on Cybernetics*, vol. 46, no. 7, pp. 1511–1523, 2016.
- [28] M. M. Ferdous, S. G. Anavatti, M. A. Garratt, and M. Pratama, "Fuzzy clustering based nonlinear system identification and controller development of pixhawk based quadcopter," in *Advanced Computational Intelligence (ICACI), 2017 Ninth International Conference on*. IEEE, 2017, pp. 223–230.
- [29] D. Dovžan, S. Blažič, and I. Škrjanc, "Towards evolving fuzzy reference controller," in *Evolving and Adaptive Intelligent Systems (EAIS), 2014 IEEE Conference on*. IEEE, 2014, pp. 1–8.
- [30] A. Zdešar, D. Dovžan, and I. Škrjanc, "Self-tuning of 2 dof control based on evolving fuzzy model," *Applied Soft Computing*, vol. 19, pp. 403–418, 2014.
- [31] A. B. Cara, L. J. Herrera, H. Pomares, and I. Rojas, "New online self-evolving neuro fuzzy controller based on the tase-nf model," *Information Sciences*, vol. 220, pp. 226–243, 2013.
- [32] H. Han, W. Zhou, J. Qiao, and G. Feng, "A direct self-constructing neural controller design for a class of nonlinear systems," *IEEE Transactions on Neural Networks and Learning systems*, vol. 26, no. 6, pp. 1312–1322, 2015.
- [33] A. B. Cara, H. Pomares, and I. Rojas, "A new methodology for the online adaptation of fuzzy self-structuring controllers," *IEEE Transactions on Fuzzy Systems*, vol. 19, no. 3, pp. 449–464, 2011.
- [34] D. Li, X. Cheng, and Z. Xu, "Gain adaptive sliding mode controller for flight attitude control of mav," *Optics and Precision Engineering*, vol. 21, no. 5, pp. 1183–1191, 2013.
- [35] X. Chen, D. Li, Z. Xu, and Y. Bai, "Robust control of quadrotor mav using self-organizing interval type-ii fuzzy neural networks (soit-ii-fnns) controller," *International Journal of Intelligent Computing and Cybernetics*, vol. 4, no. 3, pp. 397–412, 2011.
- [36] W. He, Z. Yan, and C. Sun, "Trajectory tracking control of a flapping wing micro aerial vehicle via neural networks," in *Advanced Robotics and Mechatronics (ICARM), International Conference on*. IEEE, 2016, pp. 443–448.
- [37] T. S. Clawson, S. Ferrari, S. B. Fuller, and R. J. Wood, "Spiking neural network (snn) control of a flapping insect-scale robot," in *Decision and Control (CDC), 2016 IEEE 55th Conference on*. IEEE, 2016, pp. 3381–3388.
- [38] S. Suresh and N. Sundararajan, "An on-line learning neural controller for helicopters performing highly nonlinear maneuvers," *Applied Soft Computing*, vol. 12, no. 1, pp. 360–371, 2012.
- [39] C. Dong, N. Wang, and M. J. Er, "Self-organizing adaptive robust fuzzy neural attitude tracking control of a quadrotor," in *Control Conference (CCC), 2016 35th Chinese*. IEEE, 2016, pp. 10724–10729.
- [40] A. V. Topalov and O. Kaynak, "Online learning in adaptive neurocontrol schemes with a sliding mode algorithm," *IEEE Transactions on Systems, Man, and Cybernetics, Part B (Cybernetics)*, vol. 31, no. 3, pp. 445–450, 2001.
- [41] A. V. Topalov, K.-C. Kim, J.-H. Kim, and B.-K. Lee, "Fast genetic on-line learning algorithm for neural network and its application to temperature control," in *Evolutionary Computation, 1996., Proceedings of IEEE International Conference on*. IEEE, 1996, pp. 649–654.
- [42] G. G. Parma, B. R. Menezes, and A. P. Braga, "Sliding mode algorithm for training multilayer artificial neural networks," *Electronics Letters*, vol. 34, no. 1, pp. 97–98, 1998.
- [43] S. Yu, X. Yu, and Z. Man, "A fuzzy neural network approximator with fast terminal sliding mode and its applications," *Fuzzy Sets and Systems*, vol. 148, no. 3, pp. 469–486, 2004.
- [44] G. Cascella, F. Cupertino, A. Topalov, O. Kaynak, and V. Giordano, "Adaptive control of electric drives using sliding-mode learning neural networks," in *Industrial Electronics, 2005. ISIE 2005. Proceedings of the IEEE International Symposium on*, vol. 1. IEEE, 2005, pp. 125–130.
- [45] M. O. Efe, O. Kaynak, and X. Yu, "Sliding mode control of a three degrees of freedom anthropoid robot by driving the controller parameters to an equivalent regime," *Journal of Dynamic Systems, Measurement, and Control*, vol. 122, no. 4, pp. 632–640, 2000.
- [46] E. Kayacan, E. Kayacan, H. Ramon, and W. Saeys, "Adaptive neuro-fuzzy control of a spherical rolling robot using sliding-mode-control-theory-based online learning algorithm," *IEEE Transactions on Cybernetics*, vol. 43, no. 1, pp. 170–179, 2013.
- [47] J. Kok and J. Chahl, "A low-cost simulation platform for flapping wing mavs," in *SPIE Smart Structures and Materials+ Nondestructive Evaluation and Health Monitoring*. International Society for Optics and Photonics, 2015, pp. 94 290L–94 290L.
- [48] Z. J. Wang, "The role of drag in insect hovering," *Journal of Experimental Biology*, vol. 207, no. 23, pp. 4147–4155, 2004.
- [49] —, "Dissecting insect flight," *Annu. Rev. Fluid Mech.*, vol. 37, pp. 183–210, 2005.
- [50] Z. J. Wang and D. Russell, "Effect of forewing and hindwing interactions on aerodynamic forces and power in hovering dragonfly flight," *Physical review letters*, vol. 99, no. 14, p. 148101, 2007.
- [51] G.-B. Huang, P. Saratchandran, and N. Sundararajan, "An efficient sequential learning algorithm for growing and pruning rbf (gap-rbf) networks," *IEEE Transactions on Systems, Man, and Cybernetics, Part B (Cybernetics)*, vol. 34, no. 6, pp. 2284–2292, 2004.
- [52] P. Angelov, "Fuzzily connected multimodel systems evolving autonomously from data streams," *IEEE Transactions on Systems, Man, and Cybernetics, Part B (Cybernetics)*, vol. 41, no. 4, pp. 898–910, 2011.
- [53] G.-B. Huang, P. Saratchandran, and N. Sundararajan, "A generalized growing and pruning rbf (ggap-rbf) neural network for function approximation," *IEEE Transactions on Neural Networks*, vol. 16, no. 1, pp. 57–67, 2005.
- [54] R. J. Oentaryo, M. J. Er, L. San, L. Zhai, and X. Li, "Bayesian art-based fuzzy inference system: A new approach to prognosis of machining processes," in *Prognostics and Health Management (PHM), 2011 IEEE Conference on*. IEEE, 2011, pp. 1–10.
- [55] K. S. Yap, C. P. Lim, and I. Z. Abidin, "A hybrid art-grnn online learning neural network with a  $\epsilon$  insensitive loss function," *IEEE transactions on neural networks*, vol. 19, no. 9, pp. 1641–1646, 2008.
- [56] K. S. Yap, C. P. Lim, and M. T. Au, "Improved gart neural network model for pattern classification and rule extraction with application to power systems," *IEEE transactions on neural networks*, vol. 22, no. 12, pp. 2310–2323, 2011.
- [57] E. Lughofer, "A dynamic split-and-merge approach for evolving cluster models," *Evolving Systems*, vol. 3, no. 3, pp. 135–151, 2012.
- [58] —, *Evolving fuzzy systems-methodologies, advanced concepts and applications*. Springer, 2011, vol. 53.
- [59] S. Wu, M. J. Er, and Y. Gao, "A fast approach for automatic generation of fuzzy rules by generalized dynamic fuzzy neural networks," *IEEE Transactions on Fuzzy Systems*, vol. 9, no. 4, pp. 578–594, 2001.
- [60] E. Kayacan, O. Cigdem, and O. Kaynak, "Sliding mode control approach for online learning as applied to type-2 fuzzy neural networks and its experimental evaluation," *IEEE transactions on industrial electronics*, vol. 59, no. 9, pp. 3510–3520, 2012.
- [61] V. I. Utkin, *Sliding modes in control and optimization*. Springer Science & Business Media, 2013.
- [62] E. Kayacan and R. Maslim, "Type-2 fuzzy logic trajectory tracking control of quadrotor vtol aircraft with elliptic membership functions," *IEEE/ASME Transactions on Mechatronics*, vol. 22, no. 1, pp. 339–348, 2017.
- [63] J.-J. E. Slotine, W. Li *et al.*, *Applied nonlinear control*. Prentice hall Englewood Cliffs, NJ, 1991, vol. 199, no. 1.
- [64] M. M. Ferdous, S. G. Anavatti, M. A. Garratt, and M. Pratama, "Fuzzy Clustering based Modelling and Adaptive Controlling of a Flapping

Wing Micro Air Vehicle,” in *Computational Intelligence (IEEE SSCI), 2017 IEEE Symposium Series on*. IEEE, 2017, pp. 1914–1919.

**Md Meftahul Ferdous** All about you and the what your interests are.

C:/Users/N1705848C/examples/CV-image

**Mahardhika Pratama M**